



ISSN: 0067-2904

## Magnetic Liquid Switching Using Rodlike Ferronematic 6CHBT Liquid Crystal Mixture Depending on the Diffraction Patterns

Rawa K. Ibrahim<sup>1</sup>, Aseel I. Mahmood\*<sup>1</sup>, Veronika Gdovinova<sup>2</sup>, Peter Kopcansky<sup>2</sup>

<sup>1</sup>Materials Research Directorate, Ministry of Science and Technology, Baghdad, Iraq

<sup>2</sup>Institute of Experimental Physics SAS, Watsonova 47, 040 01 Košice, Slovakia

Received: 24/8/2019

Accepted: 31/5/2020

### Abstract

Diffraction patterns formed by a ferronematic sample, which contains 4-(trans-4-n-hexylcyclohexyl)-isothiocyanatobenzene (6CHBT) liquid crystal doped with Fe<sub>3</sub>O<sub>4</sub> rodlike magnetic nanoparticles, was studied. The studied mixture can be applied as a liquid magnetic switch. The diffraction patterns were observed from the micro-lines scribed on the polymer layer, which was contained by the liquid crystal mixture cell, with dimensions of 4 nm for depth and 0.32 μm for width and 5000 line per 1 mm<sup>2</sup> in the case of absence and presence of the DC magnetic field. From the experimental results, it was observed that the application of the magnetic field caused more than 17% expansion in the diffraction patterns area at the focused point, while the number of patterns was increased by 25%. This change in the diffraction area due to the application of a magnetic field gives the motive to sense the low DC magnetic field which could be useful in the application of liquid switching.

**Keywords:** Liquid Crystal; Ferronematic; Diffraction patterns; DC low magnetic field; Liquid magnetic switch.

## المفتاح السائل المغناطيسي باستخدام خليط البلورة السائلة 6CHBT Rodlike Ferronematic اعتمادا على انماط الحيود

روى خليل. إبراهيم<sup>1</sup>, اسيل أبراهيم محمود\*<sup>1</sup>, فيرونكا كدوفينوفا<sup>2</sup>, بيتر كوبكانسكي<sup>2</sup>

<sup>1</sup>دائرة بحوث المواد، وزارة العلوم والتكنولوجيا، بغداد، العراق

<sup>2</sup>معهد الفيزياء التطبيقية، واتسنوفا، سلوفاكيا

### الخلاصة

تمت دراسة أنماط الحيود المتكونة من عينة فيروخيطية، والتي تحتوي على بلورة سائلة هي 4-(trans-4-n-hexylcyclohexyl)-isothiocyanatobenzene (6CHBT) المطعمة بأجسام نانوية مغناطيسية Fe<sub>3</sub>O<sub>4</sub>. يمكن تطبيق الخليط المدروس كمفتاح مغناطيسي سائل. حيث لوحظت أنماط الحيود في حالة وجود وعدم وجود مجال مغناطيسي نوع DC، والتي تكونت بفضل الخطوط المايكروية، المحفورة على سطح طبقة البوليمر، الموجودة في خلية خليط البلورة السائلة، وبأبعاد حفر 4 نانومتر للعمق و 0.32 ميكرومتر للعرض، و 5000 خط لكل 1 ملم<sup>2</sup>. لوحظ من النتائج التجريبية أن مساحة أنماط الحيود بوجود المجال المغناطيسي زادت بنسبة أكثر من 17% عن المساحة دون تطبيق المجال المغناطيسي في نقطة البؤرة بينما عدد الانماط زاد بنسبة 25%. أن هذا التغيير الحاصل في منطقة ظهور اهداب الحيود نتيجة تسليط المجال المغناطيسي

\*Email: aseelibrahim208@gmail.com

يعطي الدافع لاستشعار المجال المغناطيسي المنخفض DC والذي يمكن أن يكون مفيداً في تطبيق المفاتيح  
السائلة.

## Introduction

The Liquid Crystals (LCs) have very interesting properties, since some of their phases are formed at room temperature. This induced researchers to study and use these crystals in many applications due to the relatively low cost, high reliability, and the simplicity of use in devices. One of the most important findings related to the control of LCs by external fields was the threshold behaviour in the reorientation response of LCs – an effect described by Fréedericksz and named after him as the “Fréedericksz transition” [1]. The dielectric permittivity anisotropy of LCs is, in general, relatively large; thus, driving voltages of the order of a few volts are sufficient to control the orientational response. Therefore, most of the LC devices are driven by the electric field. On the other hand, because of the small value of the anisotropy of diamagnetic susceptibility ( $\chi_a = 10^{-7}$ ), the magnetic field  $H$ , that is necessary to align LC molecules, has to reach rather large values ( $B = \mu_0 H \sim 1T$ ). Therefore, LC applications using magnetic fields are rather limited. Consequently, the increase of the magnetic sensitivity of LCs is an important challenge, which can potentially broaden the area of applications and may offer an opportunity to develop new devices [2]. Brochard and de Gennes [3] first suggested theoretically the idea that could increase the magnetic sensitivity of LCs. According to them, colloidal systems called “ferronematics”, consisting of nematic LCs doped with magnetic nanoparticles in small concentrations, should respond to low magnetic fields of the order of tens of Gauss. The properties of magnetic nanoparticles significantly depend on their size, shape, and structure. Controlling the shape and the size of nanoparticles is one of the ultimate challenges in modern material research. Hence, these particles can share their properties with the host LC, enhancing the existing properties or introducing some new properties for the composite mixtures [4]. The optical properties of the Magnetic Fluid (MF) have attracted a great deal of attention of researchers. These properties include tunable refractive index [5], birefringence [6], Faraday effect [7], optical transmittance [8,9], optical scattering [10,11], and so on. Most of these are based on the fluid behaviour and magnetism of the MF. Until now, several potential applications of MF to optical devices have been proposed, such as MF optical switches [12], MF gratings [13], MF light modulation [14], MF optical fibre modulator [15], and MF optical limiting [16]. Recently, some experimental investigations about the magneto-optical effects of binary, multiple-phase, ionic, and doped MFs showed that these kinds of MFs can present some unique optical properties [5].

The diffraction optics were used here for the detection of the intensity change of the diffraction patterns due to the redistribution of patterns affected by the applied magnetic field. The diffraction patterns can be generated by several methods, such as mechanically moving wedge plates [16], tunable gratings [17], switchable gradient index lenses [18], polymer dispersed LC techniques [19,20], phase modulating using spatial light modulator (SLM) [21,22], stretchable binary Fresnel lens [23], and dual-frequency liquid crystal-based dynamic fringe pattern generator (LC-DFPG) [24]. In this work, the diffraction patterns are generated from the micro-lines scribed on the polymer layer that is sandwiched in the LC cell. The lens focal length is tuned to demonstrate the patterns by moving the white screen (diffraction patterns screen) along the Z-axis to detect the high focus intensity distribution of the transmitted light through the LC cell. The transmitted light intensity formed as patterns on the white screen is changed due to an externally applied magnetic field. There are two factors that play important roles in generating the diffraction patterns. The first is the tunable focal length of the lens, which plays an important role in achieving the high-intensity diffraction patterns and controlling the focal length with both ON and OFF settings of the applied magnetic field. The second is the micro-scribing patterns on the polymer layer that modulates the intensity distribution of the transmitted light through the LC cell (using micro-fabrication technology).

In the present work, we conducted an experimental investigation of the effect of applying a magnetic field on the diffraction pattern of modes. This work may be helpful to better understand the optical properties of nematic LC-doped MFs (ferronematic materials) and extend the applications of MFs in the optical field, especially in optical switching applications.

The ferronematic LC composite, which consists of rodlike magnetic nanoparticles were presented as a novel material that is used as a liquid magnetic switch, depending on the diffraction patterns. This allows the optical properties of ferronematic LC composite to be tuned or modulated

and creates a new class of optical devices by utilizing features of the nanomaterial scale. The diffraction process is the key to the optical control mechanisms of the order of the pattern of the light [25]. Due to the influence of the doping, the LCs with the magnetic nanoparticles  $\text{Fe}_3\text{O}_4$  will control the polarization as well as the wavefront of light through the diffraction.

Therefore, this work explores the potential of the rodlike magnetic nanoparticles in nematic LC to serve as a magnetic switch (liquid opto-magnetic switch) to make the first step (open the field) towards a truly magnetically optical switch by utilizing diffraction optics and nanotechnology.

### Experimental Work

The ferronematic samples were based on thermotropic nematic 4-(trans-4'-n-hexylcyclohexyl)-isothiocyanatobenzene (6CHBT), which was synthesized and purified at the Institute of Chemistry, Military Technical University, Warsaw, Poland. The 6CHBT is a low temperature melting enantiotropy LC with high chemical stability. The phase transition temperature from the isotropic liquid to the nematic phase was found at  $42.6^\circ\text{C}$ . Doping was done by adding nanoparticles to the LC in the isotropic phase under continuous stirring [2].

The 6CHBT LC was doped with a magnetic suspension consisting of rodlike  $\text{Fe}_3\text{O}_4$  nanoparticles coated with oleic acid as a surfactant, with volume concentration of  $2 \times 10^{-3}$ . The average diameter of rodlike particles was 16 nm and the mean length determined from the histogram of the size distribution was 70 nm. The morphology and size distribution of the prepared rodlike particles were measured by transmission electron microscopy (Tesla BS 500) and shown in Figure-1.

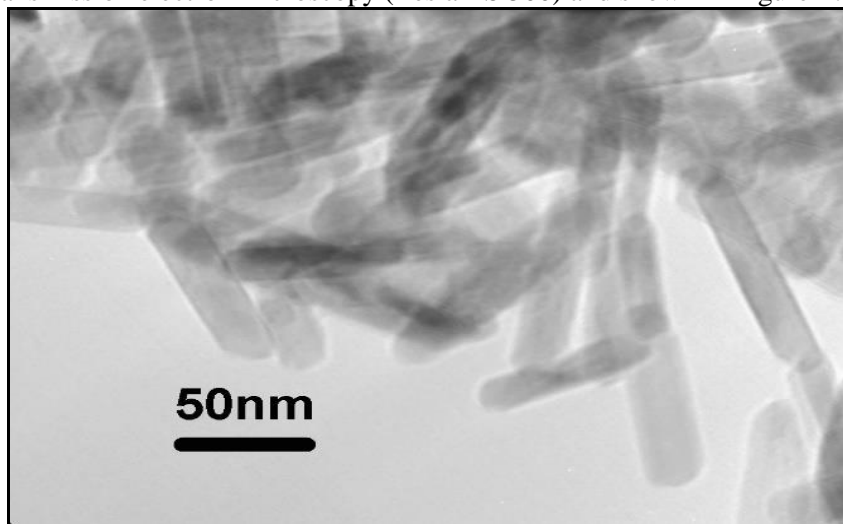


**Figure 1-** TEM image of rodlike magnetic particles.

The liquid crystal composite cell fabrication is described in a previously published work [26]. The dimensions of the cell were  $5 \times 5 \text{ cm}^2$  and the thickness was about 2 mm. The sample cell was accurately set between 'crossed' polarizers as shown in Figures- 2 and 3. The source He-Ne laser with a power of 5mW was emitting a linearly polarized light with a wavelength of 632.8 nm. The propagation direction of the incident light was normal to the applied magnetic field. The cell sample was placed inside the magnetic field in the vertical set to ensure a uniform horizontal magnetic field effect on the sample region. The strength of the magnetic field can be adjusted by tuning the magnitude of the current supply. The beam from the He-Ne laser was expanded by a beam expander (4X- Thorlabs) and then passed through an iris to reduce the optical noise so that a suitable spot size with uniform beam intensity can cover all of the cells. The light polarized with the x-axis polarizer was passed through the cell. The LC composite cell generates fringe patterns that were expanded by a projection lens (with focal length of 5 cm) and projected on a flat-panel screen. The projected fringe patterns on the flat-panel screen were captured by a CCD with 12-megapixel resolution. The photographic image and schematic setup are shown in Figures -2 and 3, respectively.

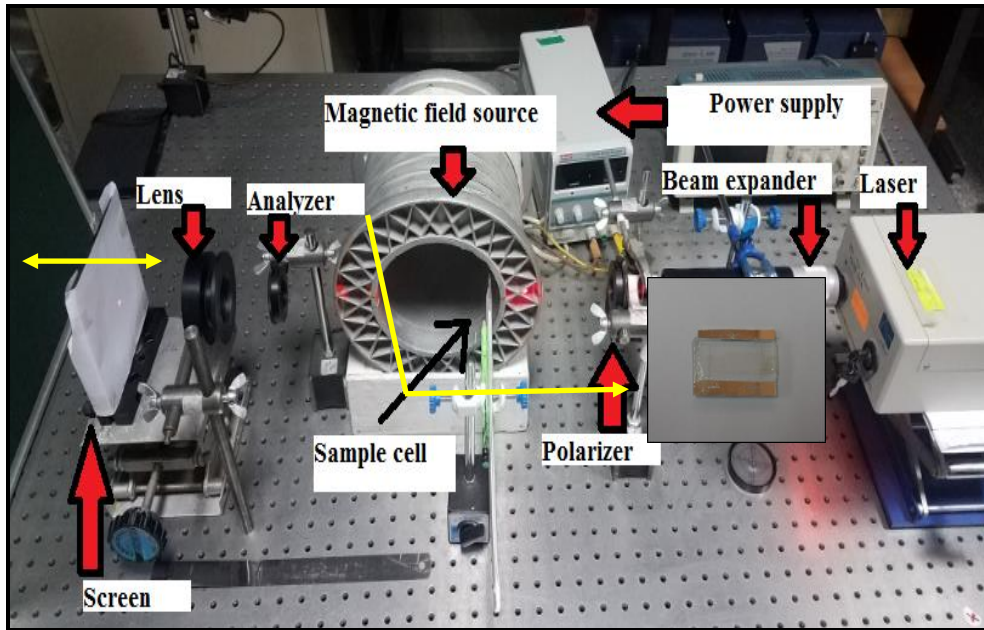


**Figure 2-** Photographic image of the optical set-up to investigate the diffraction patterns according to the application of the magnetic field, with a zoom image for the designed cell.

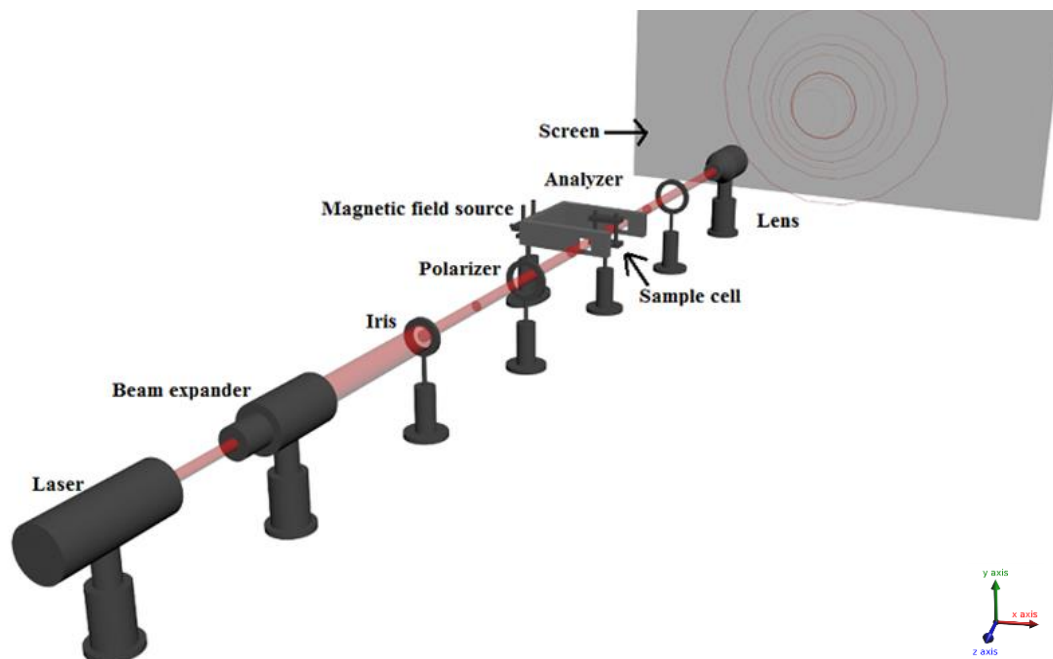


**Figure 3-** Schematic representation of the optical set-up to investigate the diffraction patterns according to the application of the magnetic field.

**Results and Discussion**

Considering the unique properties of MFs and ferronematic materials, doping MFs with nematic LCs is attractive and needs further in-depth investigation. Experimentally, we investigated the effects of applying a magnetic field on the diffraction pattern of modes.

The usage of ferronematic composite as liquid magnetic switch depends not only on the intensity of diffraction patterns but also on the lens, which possesses controlling parameters on yielding the diffraction patterns. This concurs by moving the white screen along the Z-axis in three states: before, at, and after the focus point being at the ON and OFF set of the applied magnetic field.

**Diffraction patterns before the focus point**

The white screen and then the CCD camera was located in different distances before and after the focal length of the lens (focal point 5cm) as shown in Figure-4a-d. this done for both cases the presence and absence of the magnetic field (with a maximum magnetic flux of 35 Gauss), as shown in Figure- 4a–d. For more accurate recognition and characterization, the FFT image processing was done to record the changes in the intensity and the patterns, as shown in Figure-4e-h.

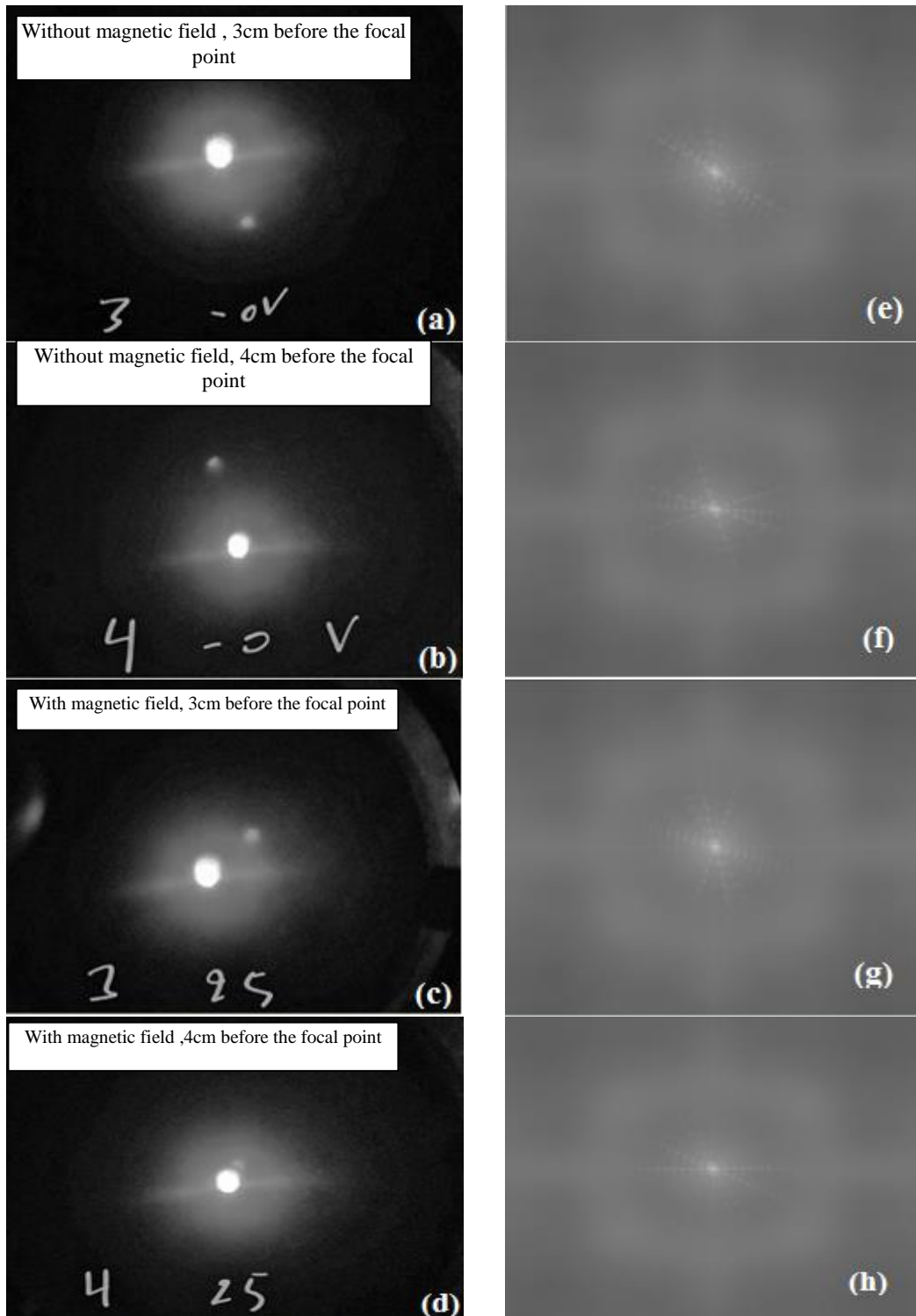


**Figure 4-** The diffraction patterns (a,b,c, and d) and the corresponding FFT images (e,f,g, and h) collected with different distance before focal length (3 and 4) cm with and without application of magnetic field.

### Diffraction patterns at the focal point

Figure- 5a,b shows the diffraction patterns formed on the white screen when the focus point was set at 5 cm for both states, i.e. the presence and absence of the magnetic field. The FFT image of patterns at the presence and absence of the magnetic field is shown in Figure- 5c,d. The figures show a slight indication about the change in the distribution of the ferroparticles under the magnetic field influence. The ferronematic molecules are electric, as well as magnetic, dipoles due to the movement of electrons. Thus, these dipoles have their magnetic field that will be influenced by the externally applied magnetic field, leading them to rearrange themselves with the direction of the applied magnetic field. The orientation coupling between the magnetic particles (their magnetic moment  $m$ ) and the LC matrix (the director  $n$ ) is strong. This coupling ensures that the effect of the magnetic field on the particles will be transferred into the nematic host [27].

The diffraction methods were utilized a useful tool for the characterization of LCs doped with rod-like magnetic particles induced by weak magnetic fields [28].

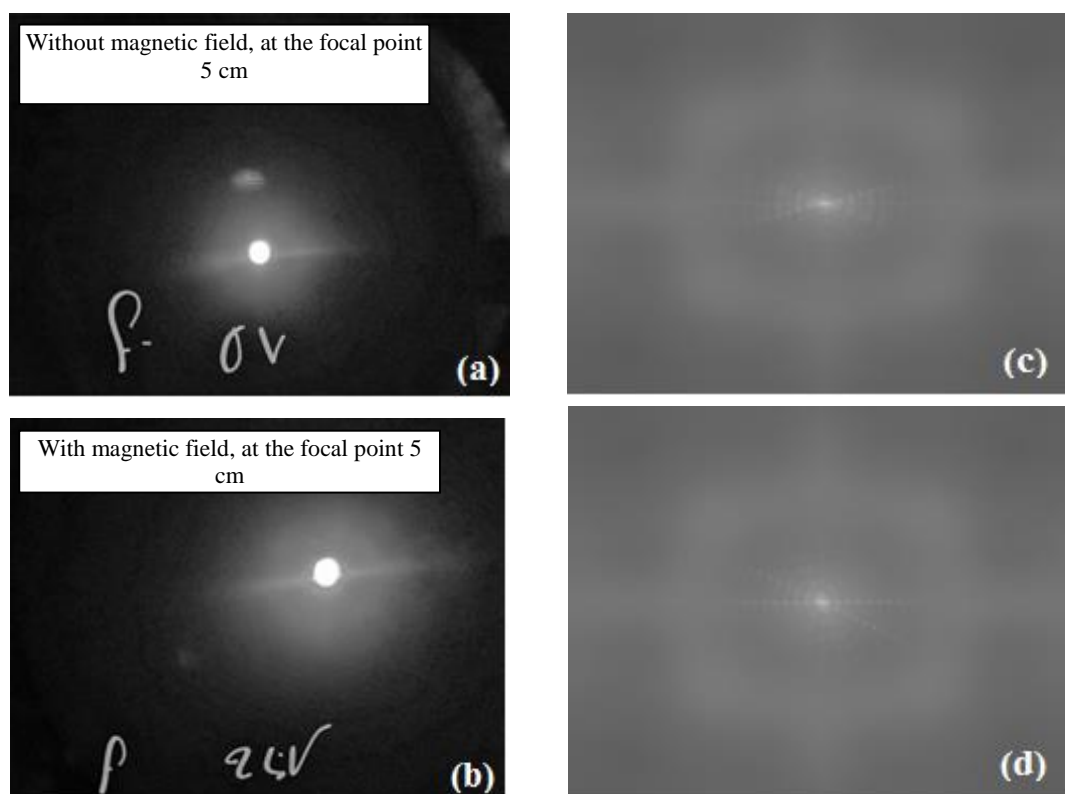


**Figure 5-** The diffraction pattern and the corresponding FFT image for spots at focal length. (a, c) without the application of a magnetic field, and (b, d) with the application of the magnetic field.

### Diffraction patterns after the focal point

The diffraction patterns formed on the white screen placed after the focus point at 6 cm and 7 cm, for both two-states of presence and absence of the magnetic field, are shown in Figure-6a–d, while the FFT images are shown in Figure- 6e-h.



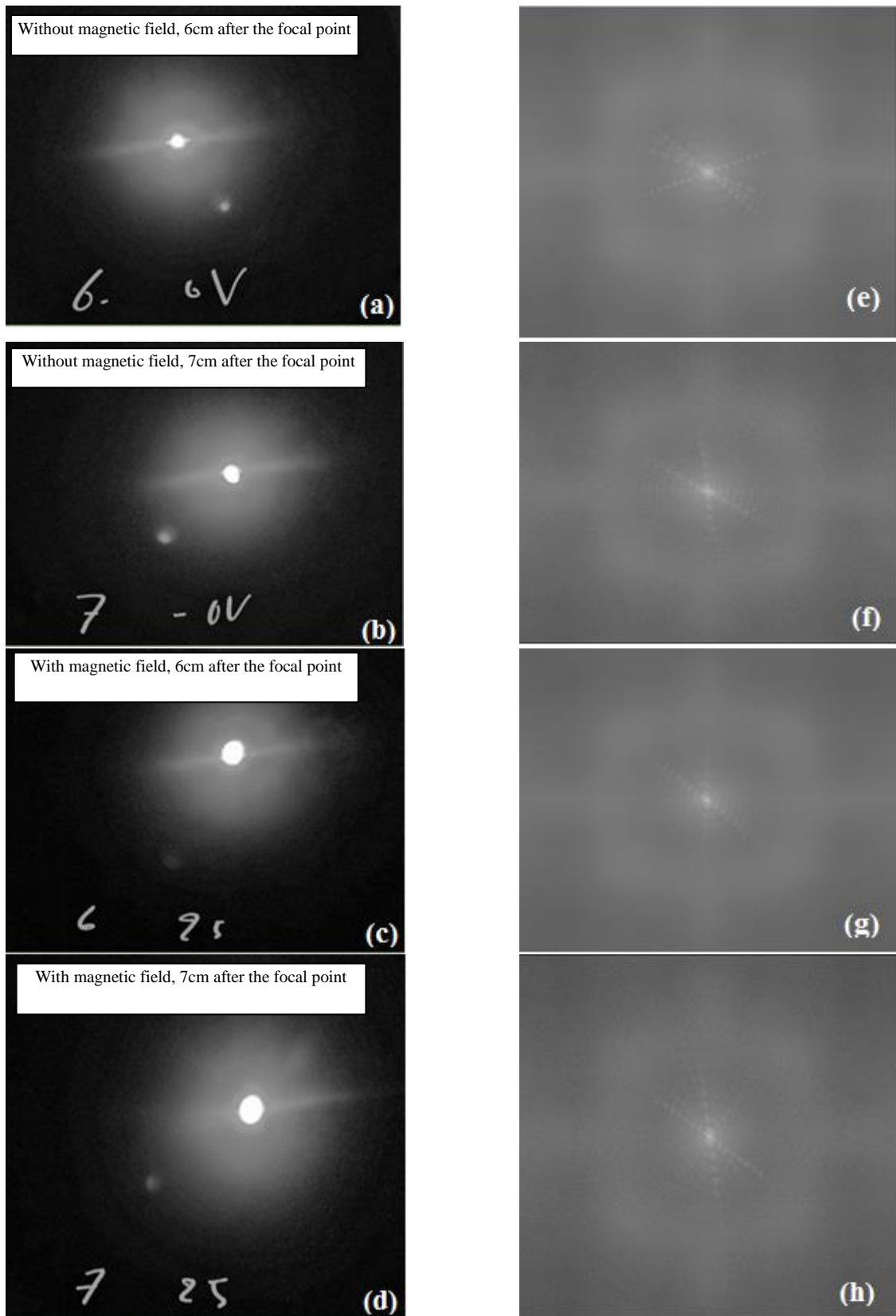


**Figure 6-** The diffraction pattern and the corresponding FFT image for spots after focal length. (a,e) and (b,f) without the application of magnetic field; (c, g) and (d, h) with the application of magnetic field.

From the previous figures, it could be summarized that, after applying the FFT filter for the above images, the intensity of the transmitted light was attenuated due to the application of the magnetic field. Some observed parameters are illustrated in Table-1 for fringes in case of the absence of the magnetic field, while Table-2 illustrates the fringes observation in the presence of the magnetic field.

**Table 1-** The behaviour of diffraction fringes in case of the absence of the magnetic field.

State	The diameter of the central fringe (mm)	No. of fringes per/cm	Order of further fringe	Visibility of fringes per cm
3 cm	2.34	4	6	1.5
4 cm	2.29	4	8	1.7
Focal point 5cm	2.85	4	6	1.4
6 cm	A=2.93 B=3.33	4	9	1.9
7 cm	2.82	4	7	1.7

**Table 2-** The behaviour of diffraction fringes in case of the presences of the magnetic field.

State	The diameter of the central fringe (mm)	No. of fringes per/cm	Order of further fringe	Visibility of fringes per cm
3 cm	2.34	4	6	1.5
4 cm	2.48	4	6	1.5
Focal point 5cm	2.38	5	8	1.7
6 cm	A=2.6 B=3.57	4	8	2

The summary from Tables-1 and 2 is that the intensity of diffraction patterns is changed after application of the magnetic field that makes the LC/magnetic particles composite work as a magnetic liquid switch to the light transmitted through the cell, based on the increase of the pattern circle diameter (area). In other words, more transmitted light gives bigger patterns circle area. The order of fringes in case of absence and presence of magnetic field was stable for 3 cm distance, then decreased to 6 for 4 cm distance. While in focal point its is increased. Then return to decrease after it. The best condition to demonstrate the magnetic liquid switch was achieved when the white screen was placed after the focal point, due to the performance of the polarized light transmitted through the cell and the phase of the liquid crystal composite.

### Conclusions

The liquid crystal 6CHBT/Fe<sub>3</sub>O<sub>4</sub> composite has novel properties, which were influenced by the applied magnetic field. Using the diffraction optics, the intensity of the patterns was changed due to the magnetic field application. The diffraction patterns area (or the pattern circle diameter) before the focused point was decreased by 13%, while the number of patterns was decreases by 33.3%. However, after the focused point, the area of diffraction patterns was expanded by 26% and the number of patterns was increased by 30%. These outcomes make the ability to set the studied ferronematic as a liquid magnetic switch depends on the intensity of the pattern. The results introduce the utilized system for much application, such as those of holograms and 3D imaging.

### Acknowledgement



This work was supported by the Slovak Research and Development Agency under the contracts Nos. 015-0453, by the Ministry of Education, Agency for Structural Funds of EU (Project ITMS 26220220012 and 26220220186), and by the Slovak Scientific Grant Agency project VEGA 2/0016/17.

## References

1. Fréedericksz V. and Zolina V. **1933**. Forces causing the orientation of an anisotropic liquid. *Trans. Faraday. Soc.*, **29**: 919–930.
2. Kopcansky P., Tomasovicova N., Toth-Katona T., Eber N., Timko M., V. Zavisova V., Majorosova J., Rajnak M., Jadzyn J. and Chaud X. **2013**. Increasing the magnetic sensitivity of liquid crystals by rod-like magnetic nanoparticles. *Magneto hydrodynamics*, **49**( 3-4): 586–591.
3. Brochard F. and De Gennes P.G. **1970**. Theory of magnetic suspensions in liquid crystals. *J. Phys. (Paris)*, **31**: 691–708.
4. Kopčanský P., Tomašovičová N., Koneracká M., Závišová V., Timko M., A. Džarová A., Šprincová A., Éber N., Fodor-Csorba K., Tóth-Katona T., Vajda A. and Jadzyn J. **2008**. Structural changes in the 6CHBT liquid crystal doped with spherical, rod-like, and chainlike magnetic particles, *Physical Review E* , **78**: 011702 –011705.
5. Pu S., Chen X., Chen Y., Liao W., Chen L. and Xia Y. **2005**. Measurement of the refractive index of a magnetic fluid by the retroreflection on the fibre-optic end face, *Applied Physics Letter*, **86**: 171904.
6. Raikher Y.L. and Stepanov V.I. **2003**. Dynamic birefringence in Ferro-colloids in crossed fields: interaction of magnetic and mechanical orientational degrees of freedom, *Colloid Journal*, **65**: 65–77.
7. Cruz J.L., Andres M.V. and Hernandez M.A. **1996**. Faraday effect in standard optical fibres: dispersion of the effective Verdet constant, *Applied Optics*, **35**: 922–927.
8. Pu S., Chen X., Chen Y., Xu Y., Liao W., Chen L. and Xia Y. **2006**. Fibre-optic evanescent field modulator using a magnetic fluid as the cladding. *Journal Applied Physics*, **99**: 093516.
9. Fang X., Xuan Y. and Li Q. **2011**. Measurement of the extinction coefficients of magnetic fluids. *Nanoscale Results Letter*, **6**: 237.
10. Mehta R.V., Patel R., Desai R., Upadhyay R.V. and Parekh K. **2006**. Experimental evidence of zero forward scatterings by magnetic spheres, *Physics Review Letter*, **96**: 127402.
11. Mehta R.V., Patel R. and Upadhyay R.V. **2006**. Direct observation of magnetically induced attenuation and enhancement of coherent backscattering of light. *Physics Review B*, **74**: 195127.
12. Yuan W., Yin C., Xiao P., Wang X., Sun J., Huang S., Chen X. and Cao Z. **2011**. Microsecond-scale switching time of magnetic fluids due to the optical trapping effect in a waveguide structure. *Microfluid Nanofluid*, **11**: 781–785.
13. Pu S., Chen X., Chen L., Liao W., Chen Y. and Xia Y. **2005**. Tunable magnetic fluid grating by applying a magnetic field. *Applied Physics Letter*, **87**: 021901.
14. Li J., Liu X., Lin Y., Bai L., Li Q., Chen X. and Wang A. **2007**. Field modulation of light transmission through ferrofluid film. *Applied Physics Letter*, **91**: 253108.
15. Pu S., Chen X., Di Z. and Xia Y. **2007**. Relaxation property of the magnetic-fluid-based fibre-optic evanescent field modulator. *Journal of Applied Physics*, **101**: 053532.
16. Saldner H. and Huntely J. **1997**. Profilometry using temporal phase and spatial light modulator-based fringe projector, *Optical Engineering*, **36**(2): 610-615.
17. Yu C., Jang E., Kim H. and Lee S. **2006**. Design and fabrication of high-performance liquid crystal gratings, *Molecular Crystal Liquid Crystal*, **454**: 765-778.
18. Kraan T., Van Bommel T. and Hikmet R.A.M. **2007**. Modelling liquid-crystal gradient-index lenses, *J. Optical Society of America A*, **24**: 3467–3477.
19. Lucchetta D.E., Karapinar R., Manni A. and Simoni F. **2002**. Phase-only modulation by nanosized polymer-dispersed liquid crystals. *Journal of Applied Physics*, **91**: 6060.
20. Ren H., Lin Y.H., Wen C.H. and Wu S.T. **2005**. Polarization-independent phase modulation of a homeotropic liquid crystal gel, *Applied Physics Letter*, **87**: 191106.
21. Hu L., Xuan L., Liu Y., Cao Z., Li D. and Mu Q.Q. **2004**. Phase-only liquid-crystal spatial light modulator for wave-front correction with high precision, *Optics Express*, **12**(26): 6403-6409.

22. Joo K.I., Park C.S., Park M.K., Park K.W., Park J.S., Seo Y., Hahn J. and Kim H.R. **2012**. Multi-spatial-frequency and phase-shifting profilometry using a liquid crystal phase modulator, *Applied Optics*, **51**(14): 2624-2632.
23. Li X., Wei L., Poelma R.H., Vollebregt S., Wei J., Urbach H.P., Sarro P.M. and Zhang G.Q. **2016**. Stretchable Binary Fresnel Lens for Focus Tuning, *Scientific Reports*, **6**(25348): 1-8.
24. Joo K.I., Kim M., Park M.K., Park H., Kim B., Hahn J., Kim H.R., **2016**. A 3D Optical Surface Profilometer Using a Dual-Frequency Liquid crystal-based Dynamic Fringe Pattern Generator, *Sensors*, **16**(11): 1-18.
25. Wilkinson T.D., Butt H., Montelongo Y., **2014**. Holographic Liquid Crystal for Nanophotonics chapter 1, edited by Q. Li, *Nanoscience with liquid crystals*, Springer Nature Switzerland AG.
26. Salman S.Ahmed, Ibrahim R.Khalil, Abdu Alsatar K.Al-Naimee, Naji A.Natic, Adnan O. Ibrahim, Majeed K.A., **2018**. Enhance the performance of liquid crystal as an optical switch by doping CdS quantum dots, IOP Conf. Series: Journal of Physics: Conf. Series **1003** 012093 doi :10.1088/1742-6596/1003/1/012093
27. Brochard F., de Gennes P.G., **1970**, Theory of magnetic suspensions in liquid crystals, *Journal de Physique*, **31**(7): 691-708.
28. Burya P., Veverička M., Kúdelčíka J., Kopčanskýb P., Timkob M., Závišová V., **2017**. Structural Changes in Liquid Crystals Doped with Rod-Like Magnetic Particles Studied by Surface Acoustic Waves, ACTA PHYSICA POLONICA A,131(4) Proceedings of the 16th Czech and Slovak Conference on Magnetism, Košice, Slovakia, June 13–17, 2016. DOI: 10.12693/APhysPolA.131.913].